RSC Advances

PAPER

View Article Online
View Journal | View Issue

Cite this: *RSC Adv.*, 2017, **7**, 48561

Novel method for the formation of monodisperse superheated perfluorocarbon nanodroplets as activatable ultrasound contrast agents†‡

C. de Gracia Lux,*[a] A. M. Vezeridis,[b] J. Lux,[a] A. M. Armstrong,[a] S. R. Sirsi,[ac] K. Hoyt[ac] and R. F. Mattrey*[a]

Microbubble (MB) contrast agents have positively impacted the clinical ultrasound (US) community worldwide. Their use in molecular US imaging applications has been hindered by their limited distribution to the vascular space. Acoustic droplet vaporization (ADV) of nanoscale superheated perfluorocarbon nanodroplets (NDs) demonstrates potential as an extravascular contrast agent that could facilitate US-based molecular theranostic applications. However these agents are metastable and difficult to manufacture with high yields. Here, we report a new formulation technique that yields reliable, narrowly dispersed sub-300 nm decafluorobutane (DFB) or octafluoropropane (OFP)-filled phospholipid-coated NDs that are stable at body temperature, using small volume microfluidization. Final droplet concentration was high for DFB and lower for OFP (>10^{12} *vs.* >10^{10} NDs per mL). Superheated ND stability was quantified using tunable resistive pulse sensing (TRPS) and dynamic light scattering (DLS). DFB NDs were stable for at least 2 hours at body temperature (37 °C) without spontaneous vaporization. These NDs are activatable *in vitro* when exposed to diagnostic US pressures delivered by a clinical system to become visible microbubbles. The DFB NDs were sufficiently stable to allow their processing into functionalized NDs with anti-epithelial cell adhesion molecule (EpCAM) antibodies to target EpCAM positive cells.

Received 14th August 2017
Accepted 10th October 2017

DOI: 10.1039/c7ra08971f

rsc.li/rsc-advances

Introduction

Owing to their increased nonlinear acoustic response compared to biological tissues, micron-scale perfluorocarbon (PFC) gas-filled microbubbles (MBs) have proven to be highly efficient ultrasound (US) contrast agents in many diagnostic and therapeutic applications, including echocardiography, vascular perfusion imaging, US-enhanced thrombolysis and drug/gene delivery across biological barriers such as the blood–brain barrier (BBB) and endothelium.[1–4] However, their relatively large size confines them to the intravascular space. When used for molecular imaging applications, they present unique challenges as they can only seek intravascular targets, are given in miniscule quantities (10^8–10^9 MBs) due to the extreme sensitivity of US to MBs, and when combined with a few minutes of circulation time, severely limits their ability to interact with receptors of interest.

Over the past two decades, researchers have evaluated the potential of converting nanoscale droplets of liquid PFC emulsion into gas-phase MBs for diagnostic and potential therapeutic uses,[5–13] image-guided and high-intensity focused ultrasound (HIFU) therapy,[14–19] drug or gene delivery,[20–25] sonoporation[26] and DNA fragmentation.[27] This conversion induced by exposure to US, is referred to as acoustic droplet vaporization (ADV),[28,29] with such US contrast agent referred to a phase-change contrast agent (PCCA). Nanoscale emulsions exhibit several advantages for molecular imaging over micron-scale MBs. Emulsion nanodroplets (NDs) have been shown to have longer *in vivo* dwell times, up to 4–5 hours in the case of dodecafluoropentane,[13,30,31] whereas MB circulation times are limited to minutes.[32] Prolonged circulation times are expected to translate to a targeting advantage of emulsions over MBs, given increased temporal and physical opportunity for ligand–receptor interaction. Emulsion NDs, up to 400 nm, are within the size regime able to extravasate into the extracellular space of

[a]*Department of Radiology, Translational Research in Ultrasound Theranostics (TRUST) Program, University of Texas Southwestern Medical Center, Dallas, TX 75390, USA. E-mail: Caroline.Lux@UTSouthwestern.edu; Robert.Mattrey@UTSouthwestern.edu; Fax: +1-214-648-5097; Tel: +1-214-648-5094; +1-214-648-5091*
[b]*Department of Radiology, University of California, La Jolla, San Diego, CA 92093, USA*
[c]*Department of Bioengineering, University of Texas at Dallas, Richardson, TX 75080, USA*

† CdGL, AMV, JL and RFM designed the experiments. CdGL, JL and AMA performed the experiments and collected the data. CdGL, JL, AMV analyzed the data and SRS, KH and RFM helped in data interpretation. CdGL, JL, SRS and RFM performed the literature review. CdGL and RFM wrote and edited the manuscript. The manuscript was written through contributions of all authors. All authors have given approval to the final version of the manuscript.

‡ Electronic supplementary information (ESI) available: Photographs of the formulation processes, additional dynamic light scattering and tunable resistive pulse sensing data. See DOI: 10.1039/c7ra08971f

tumors, with potential for nonspecific tumor targeting through the enhanced permeability and retention (EPR) effect,[33] an advantage over intravascular MBs. Emulsion NDs appear to be more resistant to US destruction than MBs, as NDs that accumulated in tumor tissue *in vivo* vaporized only in response to high intensity focused ultrasound, but not grayscale ultrasound.[34] By contrast, microbubbles are well known to be very susceptible to destruction by ultrasound imaging within clinically used ultrasound pressures.[35] Finally, the phase change of ADV holds potential for drug/gene delivery, and can be used to deliver a drug payload upon vaporization.[9]

Despite promising potential applications, certain challenges remain before successful translation and widespread use of PCCA. Specifically, emulsification of low boiling point PFCs into stable NDs is difficult and the products are typically of limited shelf-life,[36,37] prompting search for stabilizing techniques.[38] The most commonly used and favored method of producing low boiling point (<0 °C) nanodroplets of liquid decafluorobutane (DFB) (BP = −1.7 °C) or octafluoropropane (OFP) (BP = −36.7 °C) begins by producing MBs using sonication or high-speed mechanical agitation of the dispersion medium with the PFC vapor present in the headspace.[36,37,39–41] While this approach results in successful production of PCCAs, the resulting NDs have a wide size distribution requiring filtering of the final sample,[42] relatively low particle counts, and most importantly, a large number of ~100 nm-sized likely non PFC-filled liposomes that are generated during MB production and condensation. In addition, spontaneous vaporization into MBs has been reported due to thermal instability of such NDs.[37] These limitations can affect PCCAs behavior *in vivo* including circulation time, organ retention, and side effects that influences *in vivo* applications. Microfluidics has been used to generate perfluoropentane droplets with a lower size limit of approximately 7 μm and very narrow size distributions;[43] however, this approach is limited to PFCs that boil above 0 °C, low droplet production rates, large droplet sizes, and potential clogging of microfluidic channels. To enable successful translation of PCCAs, improved emulsion formulation is needed.

The objective of this study is to develop a reproducible and reliable method for manufacturing submicron-sized stable emulsions of superheated PFC with high yield and narrow size distribution. The high pressure homogenization approach proposed in this study enabled production of small and activatable DFB and OFP NDs that are stable at 37 °C temperature, and undergo US-triggered phase change at clinically relevant mechanical indices. This is the first report in which high pressure homogenization was applied to liquids with a boiling point <0 °C, enabling the formulation of reproducible high quality emulsions.

Experimental section

Materials and methods

Lipids were purchased from Avanti (Alabaster, AL) and Corden Pharma (Liestal, Switzerland). DFB and OFP were purchased from F2 Chemicals Ltd (Preston, UK). DiD, 2-iminothiolane (Traut's reagent), Zeba Spin Desalting Columns and the Measure-iTTM Thiol Assay Kit were purchased from Thermo Fisher Scientific (Rockford, IL). AffiniPure rabbit anti-mouse IgG, Fc fragment specific was purchased from Jackson ImmunoResearch (West Grove, PA, USA). Mouse anti-human CD326 (epithelial cell adhesion molecule (EpCAM)) was purchased from Bio Legend (San Diego, CA, USA). Mouse IgG was purchased from Equitech-Bio Inc. (Kerrville, TX, USA). Human breast carcinoma derived cell line SK-BR-3 were purchased from the American Type Culture Collection (ATCC; Manassas, VA, USA) and grown at 37 °C in modified McCoy's 5a medium supplemented with 10% FBS under an atmosphere of 5% CO_2. Dynamic Light Scattering (DLS) measurements were performed with a Zetasizer ZS nano-sizing system (Malvern Nano ZS, Malvern Instruments Ltd., Worcestershire, U.K.). Tunable Resistive Pulse Sensing (TRPS) measurements were performed with a qNano Gold system (Izon Science, Ltd. Cambridge, MA) using NP300 nanopores and the corresponding calibration beads. High pressure homogeinization was performed with a Low Volume Microfluidizer (LV1, Microfluidics, Westwood, MA) with a cooling coil. Vaporization experiments were performed at 8 MHz using a clinical Siemens Acuson Sequoia 512 US scanner (Siemens Medical Solutions, Mountain View, CA) equipped with a 15L8 imaging transducer. Precursor MBs prior to condensation were sized using a Multisizer 4e Coulter Counter (Beckman Coulter).

Nanodroplet formulation

A suspension of phospholipid surfactants was produced by dissolution of 1,2-distearoyl-*sn-glycero*-3-phosphocholine (DSPC) and 1,2-distearoyl-*sn-glycero*-3-phosphoethanolamine-*N*-methoxy(polyethyleneglycol)-2000 (DSPE-PEG2000) in a 9 : 1 molar ratio at a total lipid concentration of 3.5 mg mL^{-1}. The excipient solution was composed of PBS 1×, propylene glycol and glycerol in a 16 : 3 : 1 v/v/v ratio. Dry lipid film was dispersed in the excipient solution and heated at 70 °C for 15 min followed by 15 min of sonication in a bath sonicator (Branson by Thermo Fisher Scientific, Rockford, IL) at 68 °C in degassed water. The resulting sample was cooled for 2 min in a −20 °C sodium chloride/ice bath (~1 to 3 ratio by weight), transferred to a 3 mL syringe and kept in the ice bath.

DFB was condensed by flowing DFB gas into a scintillation vial cooled at −72 °C in an ethanol/dry ice bath. 150 μL of the resulting liquid DFB was added into the lipid solution and the emulsion produced through direct high pressure homogenization (9 cycles at 13 000 psi) with both coil and tray remaining cooled at −15 °C using ice and sodium chloride (~1 to 3 ratio by weight). The final emulsion was centrifuged for 2 min at 250*g* to remove any foam and then stored at 4 °C. Specific components and operating parameters as well as illustrative photographs of the formulation process are available in the ESI (Fig. S1 and S2‡).

OFP NDs were prepared using the same method with the following modifications. The excipient solution was composed of propylene glycol and PBS 1× in a 6 : 4 v/v ratio. The colloidal dispersion was cooled for 3 min in a −72 °C ethanol/dry ice bath prior to the addition of 100 μL liquid OFP that was condensed as

was done with DFB. The LV1 coil and tray were cooled to −30 °C using ice, sodium chloride, dry ice and ethanol. Illustrative photographs of the formulation process are available in the ESI (Fig. S3‡).

DFB NDs prepared by condensation were provided by Dr Sirsi following the procedure reported by Sheeran *et al.*[37] Importantly, the same lipid composition, concentration and excipient as above were used to form precursor MBs (Fig. S4A and B‡). In parallel, liposomes obtained with both techniques were prepared and used as control experiment (Fig. S4B‡). To generate those liposomes, we used the same lipid composition and excipient and used both procedures without the addition of DFB (sonication and subsequent amalgamation or high pressure homogenizer).

Preparation of DiD-labeled EpCAM-targeted DFB NDs

DiD-labeled DFB NDs were prepared by first mixing DSPC, DSPE-PEG2000, 1,2-distearoyl-*sn-glycero*-3-phosphoethanolamine-*N*-[maleimide(polyethylene glycol)-5000] (DSPE-PEG5000Mal) in a molar ratio of 9 : 0.8 : 0.2. 8 μL of a 1 mM DiD solution in ethanol was then added once the lipid suspension was clear, followed by two more min of sonication at 68 °C. The emulsion was then made using the same procedure as described above. Using the technique described by G. X. Shi *et al.*,[44] anti-Fc IgG was thiolated using Traut reagent and purified through a Zeba Spin Desalting Column. Each antibody had approximately 3 thiol groups as measured with Measure-iT™ Thiol Assay Kit. One molar equivalent of thiolated anti EpCAM antibody or non-specific IgG as control, were added to 5 × 10^{10} maleimide-terminated NDs and the mixture rotated for 1 h at room temperature on a rotating plate at 11 rpm. NDs were then washed twice by centrifugation (400*g*, 25 min, 4 °C), incubated with one molar equivalent of anti-human CD326 antibody and washed again to remove excess antibodies.

Sample sizing

DLS analysis was performed on three different emulsion samples in triplicates (9 total measurements). For each measurement, 5 μL of emulsion was diluted in 250 μL PBS 1× and transferred to a cuvette by micropipette. Droplet mean hydrodynamic diameter, distribution weighed by intensity and polydispersity index are reported. DLS covers a size range from 1 nm to 10 μm. Since the derived count rate is representative of the scattering intensity in the absence of attenuation, it allows meaningful comparison between samples as the attenuation effects of the light filters are normalized. Therefore, when the sample size is constant, constant derived count rate indicates stable concentration.

TRPS measurements, based on the Coulter principle, were performed on three emulsion samples diluted 1000 times in PBS in duplicates (6 measurements). After calibration with polystyrene beads of known size acquired from the instrument manufacturer (Izon Science), captured events are counted to yield particle count at each detected size. For these measurements we used the NP300 and NP200 nanopores that cover a size range of 85 to 900 nm, an applied stretching value of 43.8 to 45.50 mm and voltage set at 0.4–0.8 mV to keep the baseline close to 130 nA. For each measurement, the sample was analyzed at two different pressures (8 and 16 mbar) and the results averaged. Each measurement was a minimum of 500 counting events collected over a minimum of 30 s. Droplet mean and mode diameters, concentration and d_{90} are reported – d_{90} is the size below which 90% of counted particles reside.

Sample stability

After preparation, samples from each of the 3 emulsions were transferred into 3 mL glass vials with no gas headspace and stored at 4 °C. These emulsion samples were characterized by DLS and TRPS at the time of manufacture and then approximately every 3 days over 18 days in triplicates.

Three additional emulsion samples were stored at room temperature (22 °C). These samples were characterized at baseline and at 3, 27, and 50 h later.

The final three emulsion samples were heated to 37 °C and characterized by DLS and TRPS over 2 h. DLS measurements were acquired at baselines and then at 5, 15, 30, 90, and 120 min. TRPS measurements were acquired at baseline, and then at 15, 30, 60, and 120 min. Potential size, distribution and concentration changes over time were recorded. DLS was also performed at baseline and at 5 and 10 min after heating the samples to 40 °C.

The sample was monitored for microbubble formation due to thermal instability (*i.e.*, spontaneous vaporization) over 20 minutes at 37 °C. An experimental setup identical to that shown in Fig. 1 was employed, but at an *in situ* peak negative pressure (PNP) of 0.86 (sub-threshold acoustic power) and with the same ND concentration used in the acoustic droplet vaporization evaluation.

In vitro acoustic droplet vaporization

DFB ND emulsions were diluted to 1.6 × 10^9 NDs per mL into 3 mL PBS buffer in a plastic transfer pipet bulb. The bulb was placed in a tightly fitting phantom containing 0.5% corn starch acoustic scatterers in 1% agarose, and the entire assembly immersed in a heat-controlled water bath maintained at 37 °C (Fig. 1). Traditional brightness-modulated (B-mode) US imaging was performed 5 min after sample immersion using a fixed

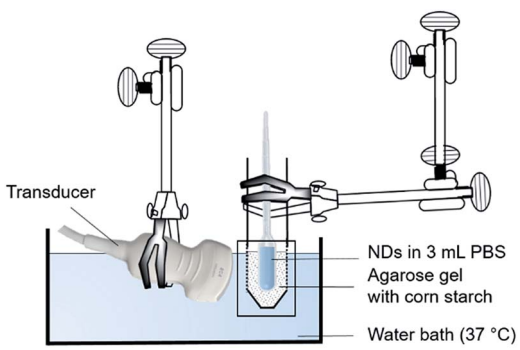

Fig. 1 Schematic representation of ultrasound (US) vaporization experimental setup.

15L8 transducer operating at 8 MHz. Temperature in bulb over time in heating bath was measured to ensure it was at 37 °C prior experiments (Fig. S5‡). The *in situ* peak negative pressure (PNP) output by the ultrasound transducer was measured using a calibrated hydrophone whose tip was placed at the electronic focus of the ultrasound transducer, 2 cm from the transducer face, where vaporization was concentrated in all of our experiments. These measurements were performed with and without the agarose/cellulose/pipette wall in the path between the transducer and hydrophone (Fig. S6‡). Samples were exposed to incremented US transmit powers from the lowest (−30 dB, onscreen MI = 0.05, PNP = 0.13 MPa) to the highest (0 dB, onscreen MI = 1.1, PNP = 2.68 MPa) while continuously capturing US images. A region-of-interest was drawn over the lumen of the bulb and mean signal intensity measured using ImageJ.[45] Experiments were done in triplicate and the mean image intensity ± standard deviation (SD) was plotted as a function of US transmit power. Vaporization threshold was defined as the power at which signal increased by >2 SD.

In vitro cell targeting

SK-BR-3 cells (5×10^5) were plated in a cell culture chamber slide (Millicell EZ SLIDES, Millipore, Billerica, MA) and 0.5 mL of McCoy's 5a medium added. Once cells were adherent, an excess of anti-human EpCAM labeled or control NDs (1×10^9) were added and allowed to incubate at room temperature for 30 min. Cells were then washed 3 times with PBS to remove unbound NDs prior to microscopy.

Results and discussion

Nanodroplet size distributions

Manufacturing DFB emulsions using a high pressure homogenizer at −20 °C yielded stable, mono-size particle emulsions with a high ND concentration (Fig. 2). DLS intensity weighted distribution showed a single peak centered at 294 ± 20 nm that was nearly normally distributed with a 0.16 PDI and slightly skewed towards smaller particles. While DLS is not useful for measuring microbubbles or multimodal particle populations, the fact that a single nearly normally distributed peak was observed suggests the absence of microbubbles in the emulsion sample (Fig. 2). Positive controls consisting of NDs in coexistence with various concentration of Definity MBs (1, 10 and 50%) confirmed that DLS pick up the peak associated with the MBs in addition to the NDs (Fig. S7‡).

The histogram ND size distribution acquired using TRPS is also shown in Fig. 2. Note that the DFB size distribution is also slightly skewed to the left with a mean diameter of 282 ± 28 nm, a d_{90} of 416 ± 71 nm, and a concentration of $1.33 \pm 0.36 \times 10^{12}$ NDs per mL.

TRPS was done with 500, 1000, 2000 and 3000 counting events (Fig. S8‡) and the fraction of the population with diameters greater than 500 nm was measured. While large droplets will likely contribute the most to thermal instability due to their lower Laplace pressure, they did not represent more than 0.9 ± 0.3% of the droplet count ($n = 3$).

Currently, the preparation of NDs by condensation of MBs is being advocated. Using this technique, the concentration of NDs samples is limited to the concentration of the precursor microbubbles (~10^9 MBs per mL). While it is well known that liposomes are generated during the production of MBs, there is no comprehensive report on their concentration. However, it is essential to evaluate the fraction of the population composed of liposomes post condensation, because those small size non echogenic liposomes will contribute to the count of sub-200 nm particles in the sample, which leads to overestimation of the ND concentration in the sample (Fig. S4‡). Manufacturing DFB emulsions using the condensation method yielded a low concentration of NDs (up to 2.7×10^9 MBs per mL in 1 mL, Fig. S4A‡) in coexistence with a high number of liposomes. The concentration of small particles (ND + liposomes) obtained by condensation was measured at 4.3×10^{11} particles per mL using TRPS (Fig. S4B‡). This concentration includes both NDs and liposomes with a maximal concentration of NDs of 2.7×10^9 NDs per mL (100% conversion of all MBs into NDs). As a control, we formulated liposomes obtained using the same technique in the absence of DFB and obtained a concentration of 6.1×10^{11} liposomes per mL, which further demonstrates that in the absence of multiple washes to isolate MBs from liposomes, the majority of small particles present in the ND sample obtained by condensation is in fact liposomes. On the other hand, liposomes formulated by high pressure homogenization (Fig. S4C‡) are sub-150 nm and do not represent a significant portion in the ND formulation. Note that in average, a concentration of 10^{12} NDs per mL was obtained for a final volume of 3 mL using our method.

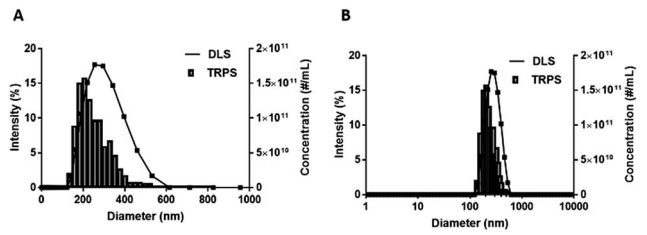

Fig. 2 Representative DFB ND emulsion size distributions measured by DLS (solid lines, intensity in %) and TRPS (histograms, concentration in NDs per mL).

Nanodroplet emulsion stability at 4 °C

Storage stability is an essential requirement for low-boiling point PFC-in-water nanoemulsions to be of practical use. Shelf-life stability was assessed with both DLS and TRPS, by monitoring ND size and concentration over 18 days of storage at 4 °C. Although MBs cannot be reliably sized using DLS because their buoyancy counteracts Brownian motion, their presence affects both the size distribution and correlation graphs. No significant change in intensity, size, derived count rate or concentration were detected over the observation period, confirming emulsion stability (Fig. 3). DLS confirmed complete absence of μm-sized particles residing between 800 nm and 10

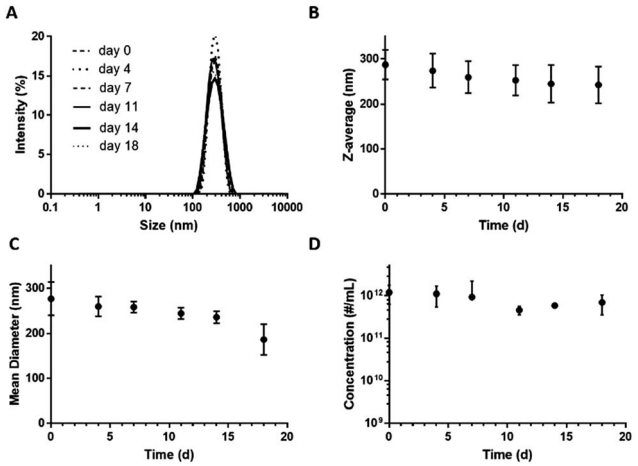

Fig. 3 Stability of DFB ND emulsions stored at 4 °C over 18 days. Size distribution (A) and *Z*-average (B) measured by DLS, and mean diameter (C) and concentration (D) measured by TRPS.

μm as well as the development of a multimodal distribution indicating that there are no MBs or large aggregates. No significant fluctuations were observed in intensity distribution, *Y*-intercept of the correlation functions, exponential decay lifetime, or emulsion characteristics from baseline values (Fig. S9‡). Further, ND emulsions withstood freezing at −20 °C without significant loss of concentration (data not shown).

Nanodroplet emulsion thermal stability

In addition to shelf-life stability we also examined DFB emulsion stability at room temperature (22 °C) over 50 h (Fig. 4A and B) and at 37 °C for 2 h (Fig. 4C and D). At room temperature, 94 ± 13%, 78 ± 15% (not statistically significant, $p = 0.2315$, based on two-tailed paired Student's *t*-test) of the ND population remain after 3 and 27 h respectively. At 37 °C, 87 ± 19%, 74 ± 28%, 71 ± 14% and 82 ± 9% of NDs remain after 15, 30, 60 and 120 min respectively (not statistically significant, $p = 0.4811$, based on two-tailed paired Student's *t*-test for 15 and 120 min).

DLS confirmed that DFB NDs exhibit optimal stability over a period of at least 2 h with no detection of particles >1 μm nor changes in size distribution (distribution weighted by intensity, volume and number) (Fig. 5A–C), and particle derived count rate (Fig. 5D). While no decrease in concentration nor changes in size were observed at 37 °C, the ND sample showed changes in shape of the correlation curve suggestive of the appearance of microbubbles and liposomes when heated to 40 °C (Fig. S10‡), most likely due to the phase-transition of the largest and least thermally stable droplets.

While DLS and TRPS confirmed stability by maintenance of size distribution and concentration, we also looked for a phase transition to occur using B-mode. When DFB NDs were exposed to a sub threshold acoustic power (onscreen MI = 0.32, measured PNP = 0.86) at 37 °C, signal intensity remained at baseline without significant vaporization (Fig. 6). As expected, only a very limited B-mode signal was observed during 20 minutes of incubation at 37 °C (mean intensity < 10 a.u. *vs.* ~125 a.u. for PNP at 2.68). This low signal was attributed to the small population of the largest droplets in the sample (the right-weighted tail in the distribution), less stable due to their lower Laplace pressure. B-mode is extremely sensitive and can detect a single microbubble. The lack of microbubble formation on B-mode over 20 minutes at 37 °C with a sub-threshold MI confirmed the thermal stability observed with DLS and TRPS.

Nanodroplet vaporization *in vitro* at 37 °C

As DFB requires more transmitted acoustic energy to vaporize *in vivo* than it does *in vitro* due to greater US attenuation by tissues, we also made emulsions of OFP that has a lower boiling point (−36.7 °C) than DFB (−1.7 °C) and should require less energy to vaporize (Fig. S11‡). DLS intensity data of OFP emulsions demonstrated a single peak centered at 203 ± 13 nm that was normally distributed with a 0.3 PDI. The OFP size distribution by TRPS was slightly skewed to the left with a mean diameter of

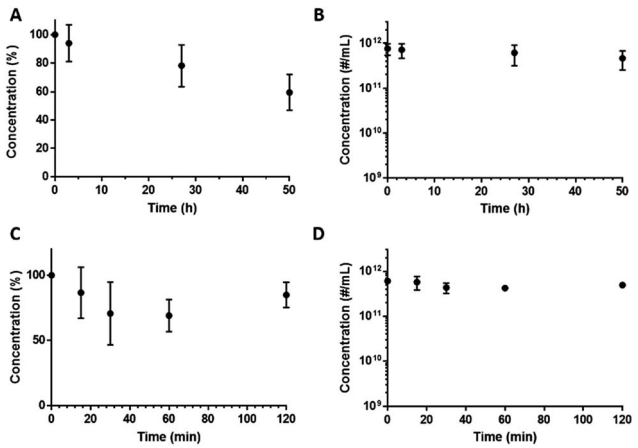

Fig. 4 NDs concentrations determined by TRPS as a function of incubation time at room temperature (22 °C) (A and B) and physiologic temperature (37 °C) (C and D).

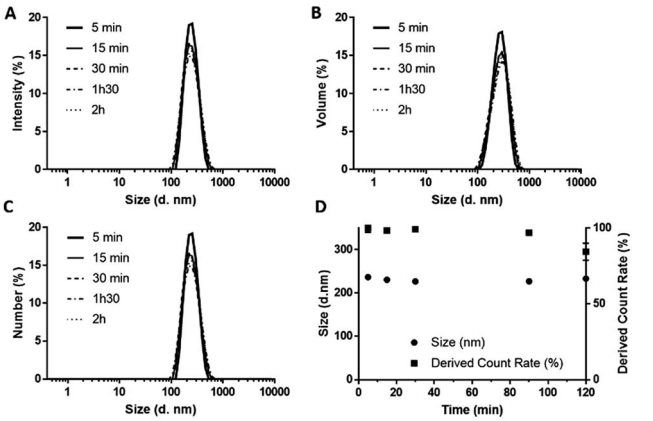

Fig. 5 Size distributions weighted by intensity (A), volume (B) and number (C), and *Z*-avg and derived count rates of NDs emulsions over 2 h incubation at 37 °C (D).

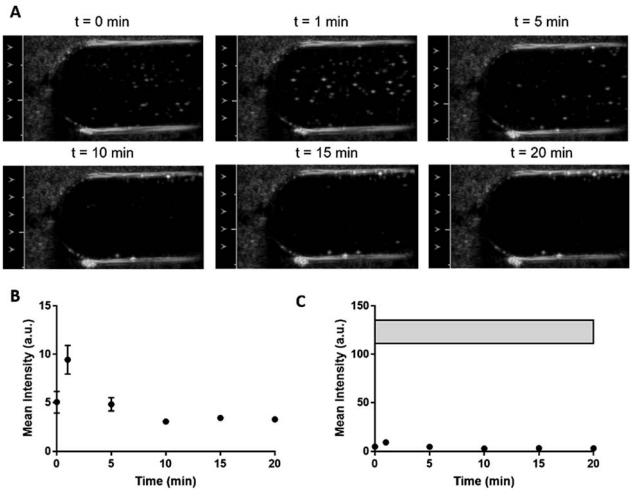

Fig. 6 Contrast enhancement of 1.6×10^9 NDs per mL DFB as a function of incubation time at 37 °C at a sub-threshold insonation (MI = 0.32, PNP = 0.86). Representative US images (A) and mean image intensity (B and C) are shown. Grey bar in (C) represent the mean image intensity range above vaporization threshold at this concentration.

182 ± 43 nm, a d_{90} of 235 ± 71 nm and a concentration of $2.0 \pm 0.17 \times 10^{10}$ NDs per mL.

When OFP and DFB NDs were exposed to increasing acoustic power at 37 °C, signal intensity remained at baseline without vaporization until the PNP passed 0.38 for OFP and 1.07 for DFB (Fig. 7). Also note that while vaporization of DFB was gradual with increasing PNP, OFP signal reached a plateau at a PNP >0.8. As expected, these results confirm that PFC boiling point influences NDs vaporization threshold. NDs obtained by the condensation method only presented a low vaporization signal at an identical concentration, which is in agreement with our hypothesis that the majority of small particles present in the ND sample is non echogenic liposomes and not NDs.

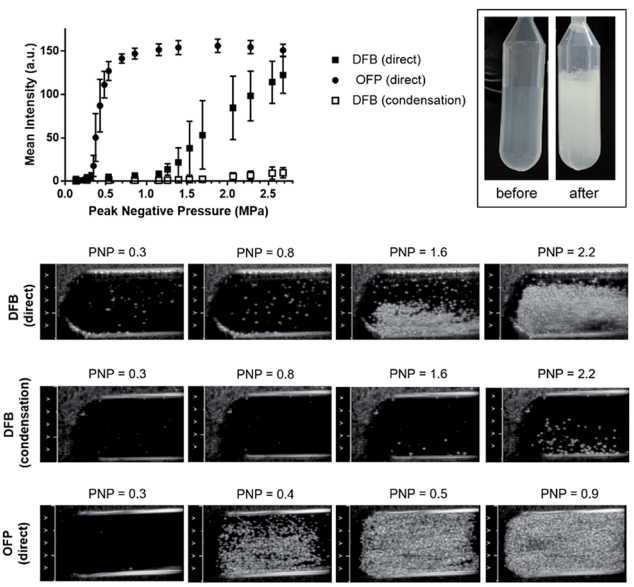

Fig. 7 Contrast enhancement of 1.6×10^9 NDs per mL DFB and 4.5×10^7 NDs per mL OFP as a function of peak negative pressure (PNP). Representative US images and mean image intensity are shown as well as photographs of the transfer pipet bulb containing DFB NDs before and after US exposure (direct). Change in sample opacity is a hallmark feature of PCCA activation. "Direct" and "condensation" refer to the direct formulation of NDs by high pressure microfluidization and condensation of preformed MBs into NDs respectively.

Nanodroplet functionalization, purification and *in vitro* targeting

A key advantage of ND formulations is their greater opportunity to target receptors *in vivo* compared to MBs because of their smaller size, larger particle count and longer circulation time. The challenge of producing targeted ND of low boiling point PFCs, is the additional time and manipulation required to attach and then wash excess ligands. We attached anti-EpCAM or non-specific IgG antibodies to DiD-labeled DFB NDs and showed by fluorescence microscopy that targeted but not control NDs bound to EpCAM positive SK-BR-3 cells (Fig. 8).

An ideal PCCA formulation should produce NDs with a vaporization threshold achievable by diagnostic clinical ultrasound systems combined with an optimal thermal stability at room and physiological temperatures to allow for practical handling and performance. The formulation and emulsification technique presented here resulted in several unique properties to achieve this goal including: (1) sub-300 nm DFB NDs with narrow size distribution (PDI < 0.2); (2) absence of MBs; (3) high ND concentration (>10^{12} NDs per mL); (4) high stability over 3 weeks at 4 °C, and over 27 h at room temperature; and more importantly, over 2 h at physiological temperature (37 °C) without measurable decrease in ND concentration. In contrast, DFB NDs made with the condensation method were reported to be unstable at 4 °C after 5 h.[37] Further, the condensation method resulted in droplets with a broad particle size

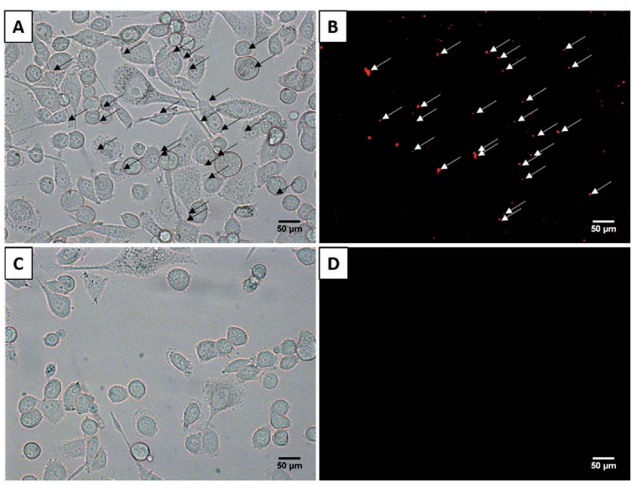

Fig. 8 Representative brightfield (A, C) and fluorescence (B, D) microscopy images show that DiD-labeled targeted DFB NDs (A, B) remained attached after washing but not control DiD-labeled NDs (C, D). Arrows pointing to DiD visible NDs in (B) are co-registered on the brightfield micrograph (A).

distribution, and low particle concentration.[37] Although the count is likely dependent on the initial MBs concentration, we speculate that the condensation method likely produces a larger number of non-PFC containing liposomes, although this possibility was not discussed or reported.

Another important distinction is that neither DFB nor OFP NDs vaporized at physiological temperature until they were exposed to ultrasound at clinically relevant power (≥0.4 MI for DFB, and ≥0.14 MI for OFP). As expected, when the NDs phase transitioned to MBs they produced a high contrast-to-noise ratio on B-mode US imaging.

A key element of the direct emulsification technique is that the resultant NDs are stable to allow further processing to produce labeled and functionalized systems, allowing the removal of non-PFC containing liposomes as well as unbound small molecules or antibodies. This purification capability assures optimal purity and paves the way for use of targeted NDs for molecular US-based theranostics. The *in vitro* results confirmed that NDs produced by direct emulsification and subsequent functionalization are able to target their intended receptors.

Conclusions

This work confirms that direct emulsification of low boiling point PFC into liquid nanodroplets for phase-shift ultrasound controlled vaporization is possible. Emulsions of DFB were stable for >18 days (entire observation periods) at 4 °C and >1 day at room temperature allowing further processing for functionalization and purification. More important, DFB formulations were stable for at least 2 h at physiologic temperature without spontaneous vaporization, allowing ample time for targeting and tissue accumulation. They transitioned into MBs *in vitro* only when exposed to ultrasound at low PNP (0.38 for OFP and 1.07 for DFB) producing marked enhancement on B-mode US imaging. We believe that these results will accelerate *in vivo* testing and translation of these promising US contrast agents.

Conflicts of interest

The authors confirm that there are no known conflicts of interest associated with this publication.

Acknowledgements

This work was supported in part by NIH grants K25EB017222 and R21CA212851 and Cancer Prevention and Research Institute of Texas (CPRIT) grant RR150010. RFM is a CPRIT Established Investigator. AMV was supported in part by NCI-5R25CA153915-03, T32-EB005970, and the Radiological Society of North America Presidents Circle Research Resident Grant RR#1472. The authors confirm that there are no known conflicts of interest associated with this publication. The authors thank Dr Rajendran Jagathesh Chandra for his help with the cell culture experiment, as well as Ridhima Chadha, Zachary Denis Juan-Sing and Sneha Rudraraju for the formulation of the NDs using the condensation method.

Notes and references

1 S. Unnikrishnan and A. L. Klibanov, *AJR, Am. J. Roentgenol.*, 2012, **199**, 292–299.
2 S. R. Sirsi and M. A. Borden, *Theranostics*, 2012, **2**, 1208–1222.
3 G. Tsivgoulis, J. Eggers, M. Ribo, F. Perren, M. Saqqur, M. Rubiera, T. N. Sergentanis, K. Vadikolias, V. Larrue, C. A. Molina and A. V. Alexandrov, *Stroke*, 2010, **41**, 280–287.
4 E. G. Schutt, D. H. Klein, R. M. Mattrey and J. G. Riess, *Angew. Chem., Int. Ed.*, 2003, **42**, 3218–3235.
5 K. Wilson, K. Homan and S. Emelianov, *Nat. Commun.*, 2012, **3**, 618.
6 T. O. Matsunaga, P. S. Sheeran, S. Luois, J. E. Streeter, L. B. Mullin, B. Banerjee and P. A. Dayton, *Theranostics*, 2012, **2**, 1185–1198.
7 T. R. Porter, C. Arena, S. Sayyed, J. Lof, R. R. High, F. Xie and P. A. Dayton, *Circulation*, 2016, **9**, 003770.
8 Y.-J. Ho and C.-K. Yeh, *Theranostics*, 2017, **7**, 1477–1488.
9 Y. Zhou, *J. Ther. Ultrasound*, 2015, **3**, 20.
10 S. Samuel, A. Duprey, M. L. Fabiilli, J. L. Bull and J. B. Fowlkes, *Microcirculation*, 2012, **19**, 501–509.
11 R. Williams, C. Wright, E. Cherin, N. Reznik, M. Lee, I. Gorelikov, F. S. Foster, N. Matsuura and P. N. Burns, *Ultrasound Med. Biol.*, 2013, **39**, 475–489.
12 N. Reznik, R. Williams and P. N. Burns, *Ultrasound Med. Biol.*, 2011, **37**, 1271–1279.
13 N. Y. Rapoport, A. M. Kennedy, J. E. Shea, C. L. Scaife and K. H. Nam, *J. Controlled Release*, 2009, **138**, 268–276.
14 X. Wang, H. R. Chen, Y. Chen, M. Ma, K. Zhang, F. Q. Li, Y. Y. Zheng, D. P. Zeng, Q. Wang and J. L. Shi, *Adv. Mater.*, 2012, **24**, 785–791.
15 C. H. Wang, S. T. Kang, Y. H. Lee, Y. L. Luo, Y. F. Huang and C. K. Yeh, *Biomaterials*, 2012, **33**, 1939–1947.
16 Y. Zhou, Z. G. Wang, Y. Chen, H. X. Shen, Z. C. Luo, A. Li, Q. Wang, H. T. Ran, P. Li, W. X. Song, Z. Yang, H. R. Chen, Z. B. Wang, G. M. Lu and Y. Y. Zheng, *Adv. Mater.*, 2013, **25**, 4123–4130.
17 P. Zhang and T. Porter, *Ultrasound Med. Biol.*, 2010, **36**, 1856–1866.
18 J. A. Kopechek, P. Zhang, M. T. Burgess and T. M. Porter, *J. Visualized Exp.*, 2012, **67**, 4308.
19 J. A. Kopechek, E. J. Park, Y. Z. Zhang, N. I. Vykhodtseva, N. J. McDannold and T. M. Porter, *Phys. Med. Biol.*, 2014, **59**, 3465–3481.
20 J. Y. Lee, C. Crake, B. Teo, D. Carugo, M. de Saint Victor, A. Seth and E. Stride, *Adv. Healthcare Mater.*, 2017, 1601246, DOI: 10.1002/adhm.201601246.
21 N. Rapoport, K. H. Nam, R. Gupta, Z. G. Gao, P. Mohan, A. Payne, N. Todd, X. Liu, T. Kim, J. Shea, C. Scaife, D. L. Parker, E. K. Jeong and A. M. Kennedy, *J. Controlled Release*, 2011, **153**, 4–15.
22 N. Rapoport, *Adv. Exp. Med. Biol.*, 2016, **880**, 221–241.
23 Y. J. Ho and C. K. Yeh, *Acta Biomater.*, 2017, **49**, 472–485.

24 M. L. Fabiilli, K. J. Haworth, I. E. Sebastian, O. D. Kripfgans, P. L. Carson and J. B. Fowlkes, *Ultrasound Med. Biol.*, 2010, **36**, 1364–1375.
25 J. Y. Lee, D. Carugo, C. Crake, J. Owen, M. de St Victor, A. Seth, C. Coussios and E. Stride, *Adv. Mater.*, 2015, **27**, 5484–5492.
26 S. M. Fix, A. Novell, Y. Yun, P. A. Dayton and C. B. Arena, *J. Ther. Ultrasound*, 2017, **5**, 1–11.
27 S. K. Kasoji, S. G. Pattenden, E. P. Malc, C. N. Jayakody, J. K. Tsuruta, P. A. Mieczkowski, W. P. Janzen and P. A. Dayton, *PLoS One*, 2015, **10**, 0133014.
28 O. D. Kripfgans, J. B. Fowlkes, D. L. Miller, O. P. Eldevik and P. L. Carson, *Ultrasound Med. Biol.*, 2000, **26**, 1177–1189.
29 C. Y. Lin and W. G. Pitt, *BioMed Res. Int.*, 2013, **2013**, 13.
30 N. Rapoport, Z. G. Gao and A. Kennedy, *J. Natl. Cancer Inst.*, 2007, **99**, 1095–1106.
31 Z. Gao, A. M. Kennedy, D. A. Christensen and N. Y. Rapoport, *Ultrasonics*, 2008, **48**, 260–270.
32 L. Mullin, R. Gessner, J. Kwan, M. Kaya, M. A. Borden and P. A. Dayton, *Contrast Media Mol. Imaging*, 2011, **6**, 126–131.
33 Y. Nakamura, A. Mochida, P. L. Choyke and H. Kobayashi, *Bioconjugate Chem.*, 2016, **27**, 2225–2238.
34 J. A. Kopechek, E. Park, C. S. Mei, N. J. McDannold and T. M. Porter, *J. Healthc. Eng.*, 2013, **4**, 109–125.
35 W. T. Shi, F. Forsberg, A. Tornes, J. Ostensen and B. B. Goldberg, *Ultrasound Med. Biol.*, 2000, **26**, 1009–1019.
36 P. S. Sheeran, S. H. Luois, L. B. Mullin, T. O. Matsunaga and P. A. Dayton, *Biomaterials*, 2012, **33**, 3262–3269.
37 P. S. Sheeran, J. D. Rojas, C. Puett, J. Hjelmquist, C. B. Arena and P. A. Dayton, *Ultrasound Med. Biol.*, 2015, **41**, 814–831.
38 Y. F. Huang, A. M. Vezeridis, J. Wang, Z. B. Wang, M. Thompson, R. F. Mattrey and N. C. Gianneschi, *J. Am. Chem. Soc.*, 2017, **139**, 15–18.
39 P. S. Sheeran, S. Luois, P. A. Dayton and T. O. Matsunaga, *Langmuir*, 2011, **27**, 10412–10420.
40 P. S. Sheeran, V. P. Wong, S. Luois, R. J. McFarland, W. D. Ross, S. Feingold, T. O. Matsunaga and P. A. Dayton, *Ultrasound Med. Biol.*, 2011, **37**, 1518–1530.
41 P. S. Sheeran, N. Matsuura, M. Borden, R. Williams, T. O. Matsunaga, P. N. Burns and P. A. Dayton, *IEEE Transactions on Ultrasonics, Ferroelectrics, and Frequency Control*, 2017, **64**, 252–263.
42 S. A. Choudhury, F. Xie, P. A. Dayton and T. R. Porter, *J. Am. Soc. Echocardiogr.*, 2017, **30**, 189–197.
43 T. D. Martz, P. S. Sheeran, D. Bardin, A. P. Lee and P. A. Dayton, *Ultrasound Med. Biol.*, 2011, **37**, 1952–1957.
44 G. X. Shi, W. J. Cui, M. Benchimol, Y. T. Liu, R. F. Mattrey, R. Mukthavaram, S. Kesari, S. C. Esener and D. Simberg, *PLoS One*, 2013, **8**, 58017.
45 J. Schindelin, C. T. Rueden, M. C. Hiner and K. W. Eliceiri, *Mol. Reprod. Dev.*, 2015, **82**, 518–529.